

Short Communication

An Anionic Non-Aqueous Single Substance Redox Flow Battery Based on Triiodide

Niklas Heiland[‡], Mathias Piescheck[‡], Uwe Schröder^{*}

Institute of Environmental and Sustainable Chemistry, Technische Universität Braunschweig, Hagenring 30, 38106 Braunschweig, Germany

*E-mail: uwe.schroeder@tu-braunschweig.de

[‡] Both authors contributed equally.

Received: 28 June 2016 / Accepted: 29 August 2016 / Published: 10 October 2016

A single-substance redox-flow battery (RFB) based on the iodide/triiodide and triiodide/iodine redox couples has been investigated. Stable charge-discharge curves were recorded under ambient air in a stirred PTFE batch cell. Current efficiencies were > 90 %. Current densities were kept low (33 $\mu\text{A cm}^{-2}$) due to high resistance (5.8 $\text{k}\Omega \text{ cm}^2$) of the cation exchange membrane used. It is shown theoretically, that the open voltage potential E_{OC} of redox flow batteries with complex stoichiometry is concentration dependent. For comproportionation electrolytes, the E_{OC} increases with bulk concentration, which is proved experimentally for the $\text{I}^-/\text{I}_3^-/\text{I}_2$ system. The open cell voltage ranged from 0.36 V to 0.58 V for 1–80 mM solutions. The formal potential difference $\Delta E^{0'}$ was determined by cyclic voltammetry (0.655 V) and open cell voltages (0.69 V), respectively. Interestingly, the calculation of $\Delta E^{0'}$ required the evaluation of the open cell voltage at a state of charge of the inverse of the golden number. This is a consequence of the “golden” stoichiometric factors of the iodide/iodine comproportionation.

To the authors' knowledge, this is the first report of a non-aqueous redox-flow battery utilizing an anionic catholyte and thus also the first where only anionic or neutral redox active species are employed.

Keywords: redox-flow battery; non-aqueous; triiodide; comproportionation; stoichiometry

1. INTRODUCTION

Redox flow batteries (RFBs) are a promising class of electrochemical energy storage devices [1–3], with the aqueous all-vanadium redox-flow battery (VRFB) being its most prominent representative [4–7]. Their design flexibility allows it to combine, in principle, any two redox couples. For liquid/liquid RFBs, this principle is narrowed by the condition that the same supporting electrolyte (solvent plus supporting salt) must be used in both half cells. This leads to the classification of aqueous

and non-aqueous RFBs, the latter referring to acetonitrile as solvent in most cases. Acetonitrile dissolves most of the studied substances and common supporting salts and is frequently chosen for its large electrochemical window, its high permittivity and low viscosity. Non-aqueous redox-flow batteries are discussed as potential alternatives to aqueous systems [8–10]. Another sensible restriction is to utilize redox active ions of like charge or neutral molecules, so that cross-mixing can be efficiently avoided by the use of ion exchange membranes. Ideally, both half cells contain the same species in different redox states, preventing irreversible capacity fade if cross-mixing occurs nonetheless. Apart from the VRFB, the design concept of a single-substance redox flow battery has been applied using transition metal complexes [11–16], redox active molecules [17,18] and polymers [19]. Both criteria (i.e. no opposite charge, same species) are met by the triiodide-based redox flow battery we report on here. To our knowledge, it is the first report of a purely anionic/neutral redox flow battery. Another all-iodine redox flow battery has been proposed previously, utilizing I_2/I^- and IO_3^-/I_2 in aqueous media. However, the concept suffered from precipitation of iodine during cycling [20]. The I_3^-/I^- couple has been successfully used as the catholyte in an aqueous zinc-iodine hybrid redox flow battery [21].

We envision several applications of the all-iodine redox flow battery within research and scientific education: 1) The system is insensitive to ambient air and uses non-hazardous, easily obtainable chemicals. These properties render it ideal for testing of equipment (e.g. cation exchange membranes in non-aqueous environment) and lab courses. 2) The I_3^-/I_2 redox couple is the first anionic/neutral catholyte ($E^0 = 0.954$ V vs. SHE [22]) to be reported for non-aqueous RFBs and can be regarded as a simpler surrogate for derivatives of 2,2,6,6-tetramethyl-1-piperidinyloxy (TEMPO) [23–26], 3,7-bis(trifluoromethyl)-N-ethylphenothiazine (BCF3EPT) [27] or 2,5-Di-*tert*-butyl-1-methoxy-4-(2'-methoxyethoxy)benzene (DBMMB) [28]. As such, it could be coupled with 9-Flourenone [28], N-methylphthalimide [25] or other widespread nitrogen containing small organic molecules which form stable anion radicals [29] to a) facilitate the full-cell study of these and b) create anionic/neutral RFBs with cell voltages above 1.5 V.

The electrochemical oxidation of iodide to iodine has been studied extensively in different media. The reaction scheme [30–32] is shown in figure 1.

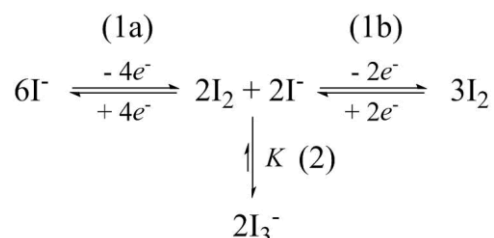


Figure 1. Simplified reaction scheme. The heterogeneous oxidation of iodide to iodine (1a) is complicated by the homogeneous comproportionation of the product with excess educt, yielding triiodide (2). Formation of iodine from triiodide takes course via the same reaction mechanism, i.e. oxidation of iodide (1b). For this, iodide has to be released from triiodide. Effectively, the competition of the second oxidation with the formation of triiodide leads to a second oxidation process. Analogous rationalizations apply to the reduction of iodine to iodide.

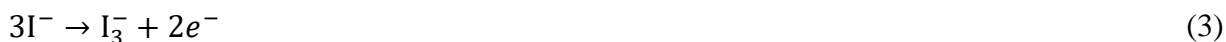
K is the stability constant of triiodide. It reflects the tendency of I^- and I_2 to comproportionate and is governed by the relative strength of solvent-solute interactions of I^- , I_3^- and I_2 [33]. If K is zero, a simple one-step two-electron reduction takes place:



With rising K , however, the mechanism is complicated by the homogeneous comproportionation of iodine and iodide:



Water is a stronger Lewis acid than acetonitrile, stabilizing iodide better [34,35]. The less polar acetonitrile stabilizes iodine better than water, as is indicated by the higher solubility. In effect, the strong water-iodide interactions shift the equilibrium (2) to the left, leading to a low K value of $10^{2.9} \text{ l mol}^{-1}$ [33,36]. In contrast, the weak donating and accepting character of acetonitrile leads to a more effective stabilization triiodide, which is expressed by relatively high K values of $10^{6.7}$ to $10^{7.3} \text{ l mol}^{-1}$. In effect, the oxidation of I^- in this solvent leads to I_3^- , rather than I_2 . The net reaction is a one-electron reaction which is facilitated by a successive chemical reaction, thus occurring at more negative potentials than $E^{0'}(I_2/I^-)$:



Further oxidation of I_3^- requires a fast reaction, which competes with the formation of I_3^- (figure 1). This is achieved at higher potentials, leading to a second voltammetric wave, corresponding to reaction (4).



It is worth noting that (1) and (2) are equivalent notations of (3) and (4), which is also expressed in the combination of the law of mass action and the Nernst equation:

$$\log K = \frac{2}{3} \cdot \frac{F}{2.3 RT} [E^0(I_2/I_3^-) - E^0(I_3^-/I^-)] \quad (5)$$

More generally, the comproportionation of product and educt of a reversible redox reaction effectively leads to a separation into two successive reactions. The resulting potential difference can be exploited for energy storage in a single-substance redox flow battery. The aim of this work is to propose and characterize a redox-flow battery based on the $I^-/I_3^-/I_2$ system for the first time. The study highlights effects of the nonunity stoichiometry on formal potentials and cell voltages which have not been considered so far.

2. EXPERIMENTAL DETAIL

2.1. Electrolyte preparation and characterization

Tetraethylammonium tetrafluoroborate (Et_4NBF_4 , Acros Organics, 99 %) was dissolved in acetonitrile (VWR Chemicals Prolabo, for HPLC) to yield a 0.1 M supporting electrolyte solution.

This solution was used to prepare the electrolytes by adding iodine (Acros Organics, 99 %+, pure) and tetraethylammonium iodide (Et_4NI , Alfa Aesar, 98 %+), respectively. Ferrocene (Aldrich, 98%) was used as an internal standard. All chemicals were used without any pretreatments and under ambient air atmosphere.

The solubility of Et_4NI was determined by cyclic voltammetry. The peak current i_p of the iodide oxidation was recorded at concentrations ranging from 20–80 mM. The resulting linear relationship between $[\text{I}^-]$ and i_p was used to extrapolate the concentration of a saturated Et_4NI solution from its measured peak current.

The conductivity of the supporting electrolyte was measured with a commercial conductivity measurement cell (TetraCon 325, WTW).

2.2. Reference electrode

The reference electrode was prepared by a procedure similar to one described elsewhere [37]. Silver iodide was precipitated on a silver wire by applying a potential of 0.2 V versus a silver wire isolated in a fritted glass tube, which contained a saturated solution Et_4NI in acetonitrile. A platinum sheet was used as counter electrode. Beforehand, the silver wire's surface was conditioned by running cyclic voltammetry 6 times between 0.7 and -0.5 V with a scan rate of 100 mV s^{-1} . The potential was applied for 2 minutes. Then the potential was changed to 0.4 V and applied for 10 minutes. After the electrochemical treatment, the wire was immersed in a saturated Et_4NI solution in a fritted glass tube which was sealed with parafilm®. The reference electrode was kept in saturated Et_4NI solution when not in use. The potential difference of two reference electrodes prepared this way was checked regularly and did not differ by more than 4 mV within 100 days. The potential of this kind of electrode was determined to be -0.904 V vs. Fc^+/Fc .

2.3. Cyclic voltammetry

A three electrode setup was utilized for the voltammetric measurements. The working electrode consisted of a shielded platinum disk (0.476 cm diameter), which was rinsed with acetonitrile before each experiment. A platinum sheet which was cleaned in a Bunsen burner flame was used as the counter electrode. The silver/silver iodide electrode described above was employed as the reference. The cyclic voltammetry measurements, as well as the charge-discharge experiments, were carried out under ambient conditions (24 °C) and air atmosphere without any pretreatments of the solutions. A VMP3 potentiostat (Biologic) was used.

2.4. Charge-discharge experiments

The charge-discharge measurements were carried out in a PTFE batch cell. The chamber was divided into two half cells by a cation exchange membrane (Ultrex CMI-7000, fumatech), which was soaked in supporting electrolyte for 48 h prior to use. Accessible membrane area was 7.8 cm^2 .

Working and counter electrode were platinum plates with a surface area of 5.13 and 4.86 cm², respectively, placed 2.8 cm apart. They were cleaned in a Bunsen burner flame before each use. Each half cell contained 12.5 ml electrolyte consisting of 0.1 M Et₄NBF₄ as the supporting electrolyte and either iodine or iodide as the electrochemical active species. The initial iodine and iodide concentrations were 10 mM during the charge-discharge cycles. Applying a constant current of 33 μA cm⁻², the cell was discharged to 0 V and charged to 0.7 V potential cutoff.

The investigation of the cell open circuit potential at different states of charge were made with 1 to 80 mM solutions of iodine and iodide. All measurements started with equimolar solutions of I⁻ and I₂, corresponding to 100 % state of charge. The solutions were permanently stirred during the measurements.

3. RESULTS AND DISCUSSION

The iodide-triiodide-iodine redox system in acetonitrile was subject of previous electrochemical studies dealing with its characterization in detail [30–32]. The cyclic voltammograms shown in figure 2 exhibit two well-defined redox processes corresponding to the I₃⁻/I⁻ and I₂/I₃⁻ couples.

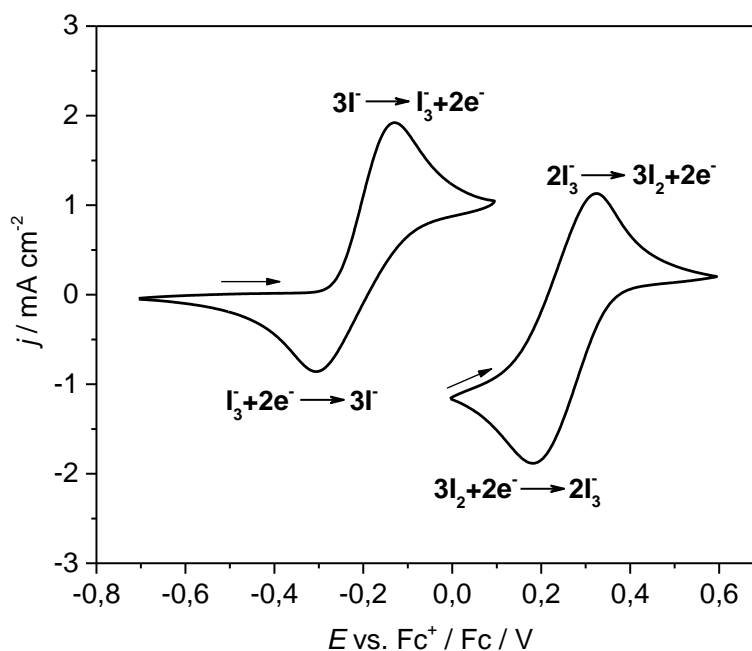


Figure 2. Cyclic voltammograms of iodide (10 mM) and iodine (10 mM) measured on a platinum disk electrode ($A = 0.178 \text{ cm}^2$), at a scan rate of 20 mV s^{-1} . Supporting electrolyte: Et₄NBF₄ (0.1 M) in acetonitrile.

The voltammetric investigation indicates chemical reversibility of both processes making this redox system suitable for RFBs. The equations added to the voltammograms equal (3) and (4). They reveal a complex stoichiometry for both redox couples. Therefore, the formal potential cannot be determined directly by simply calculating the mean value of the cyclic voltammogram's peak

potentials, i.e. the half step potential $E_{1/2}$. This parameter, however, can be converted into the formal potential $E^{0'}$ by applying a concept occasionally named as the diffusion layer method [33,38,39]. The resulting relations are [32]:

$$E^{0'}(I_2/I_3^-) = E_{1/2}(I_2/I_3^-) + a \left[\log \frac{D_{I_2}}{D_{I_3^-}} - \log[I_2]_0 + \log \frac{8}{9} \right] \quad (6)$$

$$E^{0'}(I_3^-/I^-) = E_{1/2}(I_3^-/I^-) - a \left[\log \sqrt{\frac{D_{I^-}}{D_{I_3^-}}} - 2 \log[I^-]_0 + \log \frac{4}{3} \right] \quad (7)$$

Here, $a = RT \ln 10 / zF = 0.059 / 2 V$ and D is the diffusion coefficient of the indexed species. The subscript "0" expresses the initial concentration. The calculated formal potentials are -0.340 V for I_3^-/I^- and 0.315 V for I_2/I_3^- versus Fc^+/Fc which are in good accordance with literature reports [22,33]. Consequently, the formal potential difference $\Delta E^{0'}$ is 0.655 V.

Charge-discharge measurements (figure 3 A) exhibit a uniform course of the cell potential E_{cell} over time. E_{cell} is considerably smaller than the accessible potentials of other redox systems usually used in RFBs e.g. the aqueous VRFB yielding a cell voltage of approximately 1.6 V at 100 % SoC [40] or other, non-aqueous systems [41]. The current efficiency exceeds 94 % in the first cycle and gradually decreases to a value of approximately 91 % in cycle 6. Those high values are comparable with current efficiencies achieved with VRFBs [42]. According to the voltammetric measurements shown in figure 2, the high current efficiencies indicate the absence of unwanted side reactions.

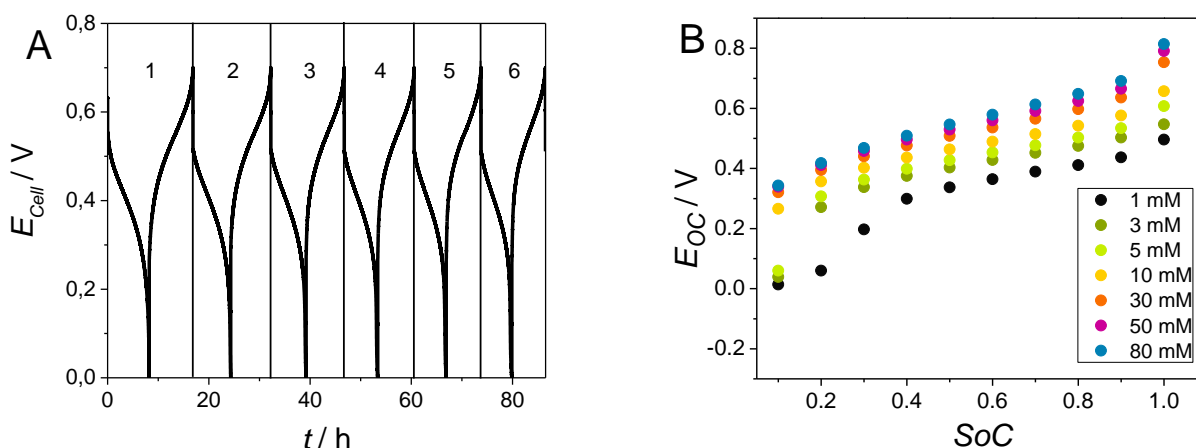


Figure 3. (A) Charge-discharge performance of a batch cell containing 10 mM iodine and 10 mM Et_4NI separated by a cation exchange membrane. Charge/discharge current were $33 \mu A cm^{-2}$. Supporting electrolyte: Et_4NBF_4 (0.1 M) in acetonitrile. (B) Cell open circuit potential versus state of charge of various, equally concentrated solutions of iodine and iodide. Supporting electrolyte: Et_4NBF_4 (0.1 M) in acetonitrile.

Furthermore, a capacity loss per cycle can be observed. The loss is 9 % in cycle 2 and steadily decreases to approximately 3 % in the last cycle. One possible reason may be the tendency of the used solutions to ascend and pass small gaps due to low viscosity of acetonitrile and the resulting strong adhesive force. This process, albeit relatively slow, causes the substances to leave the cell. Moreover,

small amounts of the redox active species may pass through the membrane causing a slight self-discharge effect.

From figure 3 A, the ohmic drop is read to be about 0.2 V, which corresponds to a cell resistance of about $R_{cell} = 6100 \Omega \text{ cm}^2$. The conductivity of the supporting electrolyte is 10 mS cm^{-1} . With the given cell geometry, the resistance of the unstirred electrolyte is in the order of $R_{el} = 300 \Omega \text{ cm}^2$. Thus, the cell resistance can be largely attributed to the membrane resistance, which is estimated to be $R_{mem} \approx R_{cell} - R_{el} = 5800 \Omega \text{ cm}^2$. For small overpotentials, the charge transfer resistance R_{CT} can be calculated from the exchange current density using $R_{CT} = RT/Fj_0$. Employing $j_0 = 2 \times 10^3 \text{ A cm}^{-2}$ as a mean exchange current density for the electrochemical reactions involved [32], this yields $R_{CT} \approx 1.3 \times 10^{-5} \Omega \text{ cm}^2$. Thus, the $\text{I}^-/\text{I}_3^-/\text{I}_2$ RFBs is far from being limited by the electrode kinetics in the present setup.

Figure 3 B reveals that the open cell potential depends on the concentration of the redox electrolytes. This can be rationalized by the following consideration: According to equations (3) and (4), the Nernst equations for both redox couples are as follows:

$$E(\text{I}_2/\text{I}_3^-) = E^{0'}(\text{I}_2/\text{I}_3^-) + a \log \left(\frac{[\text{I}_2]_{\text{I}_2}}{[\text{I}_3^-]_{\text{I}_2}^2} \right) \quad (8)$$

$$E(\text{I}_3^-/\text{I}^-) = E^{0'}(\text{I}_3^-/\text{I}^-) + a \log \left(\frac{[\text{I}_3^-]_{\text{I}^-}}{[\text{I}^-]_{\text{I}^-}^3} \right) \quad (9)$$

The subscripts of the triiodide concentrations refer to the corresponding partner of the redox couple. The iodine and iodide concentrations can be expressed with the state of charge (*SoC*). The concentrations of I_2 and I^- are equal at all times, which is expressed in a common concentration c here. The *SoC* is then:

$$\text{SoC} = \frac{[\text{I}_2]}{[\text{I}_2]_0} = \frac{[\text{I}^-]}{[\text{I}^-]_0} = \frac{c}{c_0} \quad (10)$$

The triiodide concentrations of both half cells differ from each other, since the triiodide formation per molecule iodine is twice the formation per iodide molecule. Expressing the triiodide concentration with the iodine and iodide concentrations, it follows:

$$[\text{I}_3^-]_{\text{I}_2} = \frac{2}{3}(c_0 - c) \quad (11)$$

$$[\text{I}_3^-]_{\text{I}^-} = \frac{1}{3}(c_0 - c) \quad (12)$$

Combining (8) and (9) with (10), (11) and (12) leads to:

$$E(\text{I}_2/\text{I}_3^-) = E^{0'}(\text{I}_2/\text{I}_3^-) + a \left[2 \log \frac{3}{2} + \log \frac{c_0 \text{SoC}^3}{(1 - \text{SoC})^2} \right] \quad (13)$$

$$E(I_3^-/I^-) = E^{0'}(I_3^-/I^-) + a \left[\log \frac{1}{3} + \log \frac{1 - SoC}{c_0^2 SoC^3} \right] \tag{14}$$

Therefore, the open cell voltage E_{OC} can be written as:

$$E_{OC} = E(I_2/I_3^-) - E(I_3^-/I^-) = \Delta E^{0'} + a \log \frac{27}{4} + 3a \log \frac{SoC^2}{1 - SoC} + 3a \log c_0 \tag{15}$$

Equation (15) describes the course of the cell open circuit voltage shown in figure 3 B. It also explains the observable concentration dependence of the cell voltage. Consequently, the cell voltage can be tuned to a certain extend by varying the employed amount of substance. Obviously, this effect is capped by the component with the lowest solubility. In the case mentioned here, the solubility of Et_4NI constitutes the limit. The maximum solubility was determined to be approximately 87 mM in acetonitrile containing 0.1 M Et_4NBF_4 .

In order to detect deviations from the Nernstian behavior, the E_{OC} data of figure 3 B is plotted against $\log(SoC^2/(1 - SoC))$ in figure 4 A, which represents a linear form of equation (15). At low concentrations, it can be observed that the logarithmic trend fades inexplicably below 40 % SoC . Therefore, only the linear portions of the graphs (framed in figure 4 A) are suitable for a linear regression.

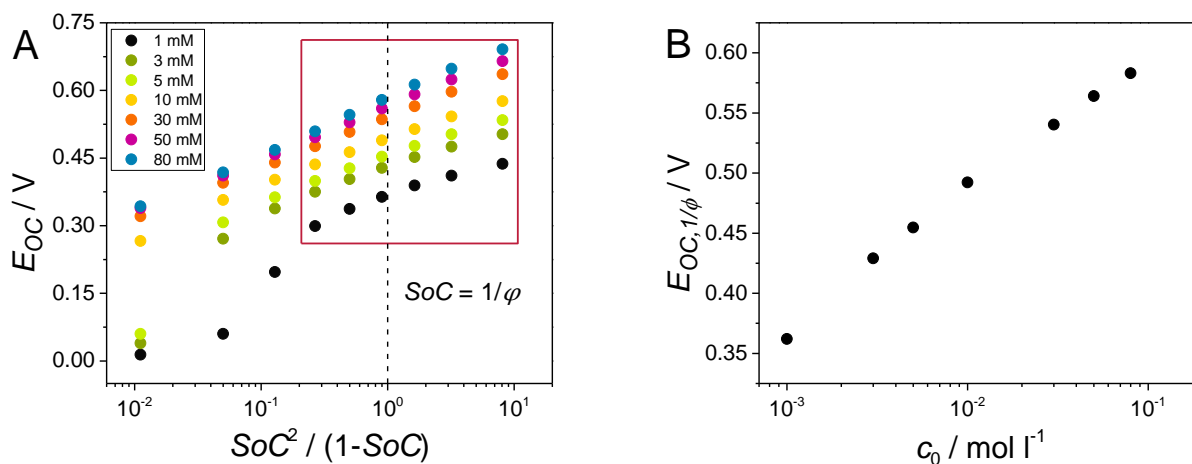


Figure 4. (A) Linearized plot of the cell open circuit potential, corresponding to equation (16). The framed portions of the graphs were utilized for linear regressions. The dashed line indicates the position of the y-intercept. (B) Linearized plot of the interpolated y-intercept determined from the data shown in figure 4 A, as given by equation (17).

The y-intercept of equation (15) occurs at

$$\log \frac{SoC^2}{1 - SoC} = 0 \quad \leftrightarrow \quad SoC = \frac{-1 + \sqrt{5}}{2} = \frac{1}{\varphi} \approx 0,618 \tag{17}$$

where φ is the *golden number*. It can be shown that only “golden” stoichiometries with $2 \sum_i \nu_i = \sum_j \nu_j$, where ν_i and ν_j are the stoichiometric factors of the educts and products, respectively,

cause this curiosity to occur. At a state of charge of $1/\varphi$, the *SoC* itself has no contribution to the cell voltage and equation (15) is reduced to

$$E_{OC,1/\varphi} = \Delta E^{0'} + a \log \frac{27}{4} + 3a \log c_0 \quad (18)$$

$\Delta E_{1/\varphi}$ was read from the linear fit and plotted against $\log c_0$ (figure 4 B). The y-intercept of a linear regression of this plot delivered the formal potential difference $\Delta E^{0'} = 0.69$ V. This is in good agreement with the result obtained by using the diffusion layer method (0.655 V).

However, the equations (6) and (7) based on the diffusion layer method imply a concentration dependence of the formal potentials $E^{0'}$. The diffusion layer method was derived only for pure solutions [38,39], therefore it cannot be used to describe *SoC*-dependent potentials. Nonetheless, one would expect that $\Delta E^{0'}$ changes with both c_0 and *SoC*, since varying *SoC* is equivalent to varying concentrations, even though this is generally not considered.

In contrast, the formal evaluation of the charge-discharge curves (equations (8) to (18)) had to be done under the assumption of a constant $E^{0'}$. Inserting equations (6) and (7) into (8) and (9) would not have been legitimated, since the first two only apply at 0 and 100 % *SoC*, while the latter are not defined at these states. It was found that the charge-discharge measurements show Nernstian behavior at higher *SoC*. Hence, in this regime, equation (18) was applicable and $\Delta E^{0'}$ could be extracted.

As a conclusion, two methods which cannot be compared in strict manner were used to calculate $\Delta E^{0'}$. This was possible because different assumptions have been made to elude the concentration dependency of $\Delta E^{0'}$. Both methods gave similar results, suggesting that this is a viable way to compare cyclic voltammetry and charge-discharge data in a quantitative way.

4. CONCLUSIONS

In this work, a non-aqueous redox flow battery based on the comproportionation of iodine and iodide to triiodide has been studied. Cyclic voltammetry as well as charge-discharge measurements revealed a chemically highly reversible behavior of the studied system. The complex stoichiometry of the electrochemical reactions led to two interesting effects.

First, conventional methods of the formal potential determination could not be applied. Two alternative approaches were used and proved to yield similar results: The diffusion layer method based on cyclic voltammetry data and the evaluation of open cell voltages at $SoC = 1/\varphi$. The curious occurrence of the golden number φ is a direct consequence of the “golden” stoichiometry.

Second, the cell voltage depends on the concentration of the iodide/iodine system employed. This finding highlights the role of redox electrolytes based on comproportionation with non-unity stoichiometry. Spontaneous charge recombination, a single redox active moiety and increasing cell voltages with increasing concentration are inherent features of this class of reactions, which are favorable for redox-flow batteries. Nonetheless, in the case of the all-iodine RFB, the overall cell voltage remains small, rendering it a less efficient energy storage system than competing electrolytes. However, its insensitivity to air and water, its simplicity, the cost efficiency as well as the

harmlessness of the used substances make this system very suitable for education. Further applications include the study of cation exchange membranes and anionic anolytes in non-aqueous environments. The study of alternative membranes as well as more soluble iodide salts appear to be fruitful continuations of this work.

ACKNOWLEDGEMENTS

N. Heiland thanks Deutsche Bundesstiftung Umwelt (DBU) for granting a PhD scholarship.

References

1. J. Noack, N. Roznyatovskaya, T. Herr and P. Fischer, *Angewandte Chemie (International ed. in English)*, 54 (2015) 9776.
2. P. Leung, X. Li, C. Ponce de León, L. Berlouis, C. T. J. Low and F. C. Walsh, *RSC Adv.*, 2 (2012) 10125.
3. F. Pan and Q. Wang, *Molecules (Basel, Switzerland)*, 20 (2015) 20499.
4. G. Kear, A. A. Shah and F. C. Walsh, *Int. J. Energy Res.*, 36 (2012) 1105.
5. C. Ding, H. Zhang, X. Li, T. Liu and F. Xing, *J. Phys. Chem. Lett.*, 4 (2013) 1281.
6. A. Parasuraman, T. M. Lim, C. Menictas and M. Skyllas-Kazacos, *Electrochimica Acta*, 101 (2013) 27.
7. M. Skyllas-Kazacos, L. Cao, M. Kazacos, N. Kausar and A. Mousa, *ChemSusChem*, 9 (2016) 1521.
8. K. Gong, Q. Fang, S. Gu, Li, Sam Fong Yau and Y. Yan, *Energy Environ. Sci.*, 8 (2015) 3515.
9. R. M. Darling, K. G. Gallagher, J. A. Kowalski, S. Ha and F. R. Brushett, *Energy Environ. Sci.*, 7 (2014) 3459.
10. Y. Huang, S. Gu, Y. Yan and Li, Sam Fong Yau, *Current Opinion in Chemical Engineering*, 8 (2015) 105.
11. M. H. Chakrabarti, R. A. W. Dryfe and E. . Roberts, *Electrochimica Acta*, 52 (2007) 2189.
12. Q. Liu, A. A. Shinkle, Y. Li, C. W. Monroe, L. T. Thompson and A. E. Sleightholme, *Electrochemistry Communications*, 12 (2010) 1634.
13. Q. Liu, A. E. Sleightholme, A. A. Shinkle, Y. Li and L. T. Thompson, *Electrochemistry Communications*, 11 (2009) 2312.
14. A. E. Sleightholme, A. A. Shinkle, Q. Liu, Y. Li, C. W. Monroe and L. T. Thompson, *Journal of Power Sources*, 196 (2011) 5742.
15. P. J. Cappillino, H. D. Pratt, N. S. Hudak, N. C. Tomson, T. M. Anderson and M. R. Anstey, *Adv. Energy Mater.*, 4 (2014) n/a.
16. T. Herr, P. Fischer, J. Tübke, K. Pinkwart and P. Elsner, *Journal of Power Sources*, 265 (2014) 317.
17. P. G. Rasmussen, *Electrical storage device utilizing pyrazine-based cyanoazacarbons and polymers derived therefrom*, [https://www.google.com/patents/US8080327\(US 8080327 B1\)](https://www.google.com/patents/US8080327(US 8080327 B1) (20.12.2011)) (20.12.2011).
18. R. Potash, J. R. Mckone, H. D. Abruna and S. Conte, *Symmetric redox flow battery containing organic redox active molecule*, [http://google.com/patents/WO2015148357A1?cl=no\(WO2015148357 A1\)](http://google.com/patents/WO2015148357A1?cl=no(WO2015148357 A1) (2015)) (2015).
19. J. H. Yang, J.-D. Jeon and J. Shim, *Meeting Abstracts*, MA2014-01 (2014) 251.
20. M. Skyllas-Kazacos and N. Milne, *J Appl Electrochem*, 41 (2011) 1233.

21. B. Li, Z. Nie, M. Vijayakumar, G. Li, J. Liu, V. Sprenkle and W. Wang, *Nature communications*, 6 (2015) 6303.
22. J. Datta, A. Bhattacharya and K. K. Kundu, *Bull. Chem. Soc. Jpn.*, 61 (1988) 1735.
23. S.-K. Park, J. Shim, J. Yang, K.-H. Shin, C.-S. Jin, B. S. Lee, Y.-S. Lee and J.-D. Jeon, *Electrochemistry Communications*, 59 (2015) 68.
24. T. Liu, X. Wei, Z. Nie, V. Sprenkle and W. Wang, *Adv. Energy Mater.* (2015).
25. Z. Li, S. Li, S. Liu, K. Huang, D. Fang, F. Wang and S. Peng, *Electrochem. Solid-State Lett.*, 14 (2011) A171.
26. X. Wei, W. Xu, M. Vijayakumar, L. Cosimbescu, T. Liu, V. Sprenkle and W. Wang, *Adv. Mater.*, 26 (2014) 7649.
27. A. P. Kaur, N. E. Holubowitch, S. Ergun, C. F. Elliott and S. A. Odom, *Energy Technology*, 3 (2015) 476.
28. X. Wei, W. Xu, J. Huang, L. Zhang, E. Walter, C. Lawrence, M. Vijayakumar, W. A. Henderson, T. Liu, L. Cosimbescu, B. Li, V. Sprenkle and W. Wang, *Angew. Chem.* (2015) 8808.
29. R. S. Assary, F. R. Brushett and L. A. Curtiss, *RSC Adv*, 4 (2014) 57442.
30. C. L. Bentley, A. M. Bond, A. F. Hollenkamp, P. J. Mahon and J. Zhang, *J. Phys. Chem. C*, 118 (2014) 22439.
31. R. Guidelli and G. Piccardi, *Electrochimica Acta*, 12 (1967) 1085.
32. V. A. Macagno, M. C. Giordano and A. J. Arvía, *Electrochimica Acta*, 14 (1969) 335.
33. C. L. Bentley, A. M. Bond, A. F. Hollenkamp, P. J. Mahon and J. Zhang, *J. Phys. Chem. C*, 119 (2015) 22392.
34. I. V. Nelson and R. T. Iwamoto, *Journal of Electroanalytical Chemistry (1959)*, 7 (1964) 218.
35. R. T. Iwamoto, *Anal. Chem.*, 31 (1959) 955.
36. R. W. Ramette and R. W. Sandford, *J. Am. Chem. Soc.*, 87 (1965) 5001.
37. A. W. Hassel, K. Fushimi and M. Seo, *Electrochemistry Communications*, 1 (1999) 180.
38. M. S. Shuman, *Anal. Chem.*, 41 (1969) 142.
39. A. Jaworski, M. Donten, Z. Stojek and J. G. Osteryoung, *Anal. Chem.*, 71 (1999) 243.
40. M. Skyllas-Kazacos, M. H. Chakrabarti, S. A. Hajimolana, F. S. Mjalli and M. Saleem, *J. Electrochem. Soc.*, 158 (2011) R55-R79.
41. S.-H. Shin, S.-H. Yun and S.-H. Moon, *RSC Adv.* (2013).
42. L. Li, S. Kim, W. Wang, M. Vijayakumar, Z. Nie, B. Chen, J. Zhang, G. Xia, J. Hu, G. Graff, J. Liu and Z. Yang, *Adv. Energy Mater.*, 1 (2011) 394.